Pramāṇa - J. Phys., Vol. 33, No. 1, July 1989, pp. 21–32. © Printed in India.

Shell structure in deformed nuclei and nuclear fission

V M STRUTINSKY
Institute for Nuclear Research, Prospekt Nauki 47, 252028, Kiev-28, USSR

Abstract. Some new aspects in the theory of heavy nuclei emerging from studies of nuclear shell structure in the nuclear-fission process are described. Specific subjects cover general understanding of shell structure, the significance of macroscopic modes and the droplet model.

Keywords. Shell structure; deformed nuclei; nuclear fission; macroscopic mode; droplet model.

PACS No. 21·60

1. Introduction

The process of nuclear fission proved to be a very firm testing ground for checking our basic understanding of nuclear processes involving significant variations of nuclear shape, finite velocity of deformation and, in general, a significant redistribution of the nuclear constituents. The process of formation of a theory of heavy-ion collisions is in many respects based upon experimental and theoretical fission studies. It is the author's firm belief that fission will again be in the centre of attention for nuclear physicists when the predictions of the new theory are checked, since it is difficult to find another process that has been studied so thoroughly and yet is so demanding as nuclear fission.

This paper reviews some points which have arisen from a study of various shell phenomena in deformed nuclei and in fission within a theoretical approach known as the shell correction method. It may demonstrate the variety of problems arising in the theory of the fission process. The somewhat arbitrary selection of topics reflects the author's intention to summarize those aspects of nuclear theory where the study of shell structure effects in fission has contributed most significantly. It turned out that the progress made in solving these problems was also closely related to a better understanding of the first principles of the combined macroscopic-microscopic approach, thus showing that the subjects are closely interwoven.

The first general question resulting from the many numerical investigations (Nilsson *et al* 1969; Brack M *et al* 1972; Nix 1972) of the shell structure in strongly deformed nuclei was: Why is the shell structure so widely applicable? or:

2. What is shell structure?

The calculations with a variety of single-particle potentials—realistic and not quite so realistic—have disclosed that the characteristic feature of nuclear shell structure—the relatively regular structure of single-particle level bunching—was a property common to all single-particle spectra. Only by way of exceptions were relatively smooth distributions of single-particle energies obtained, and it was then suspected that one was dealing with some general feature of the eigenvalue distributions whose description was, however, missing in the textbook references.

Phenomenologically, the nucleon shell structure in heavy nuclei plays a role which, in very many respects, is analogous to that of the band structure of electron spectra in solid-state physics: as in crystals, bands of allowed and forbidden energies exist. The unfilled band—or shell—leads to an increase in susceptibility and, therefore, to decreased stability of the nucleus in the given state. In contrast, the filled band—or the magic nucleus—is characterized by an increased stability. The appearance of the nuclear band structure is even more dramatic because, as it has turned out, the specific distribution of the nucleon shells—or the bands—depends significantly on the shape of the nuclear surface, which is the least stiff one among all nuclear collective degrees of freedom. The distortion of the nuclear shape redistributes the shells, and the stability conditions vary in the process of deformation. The result is the appearance of stable deformed shapes of some nuclei and the double-, or, possibly, even more often humped fission barriers.

After these computer-based findings we are naturally inclined to look for a general theory to explain the origin of such phenomena in nuclei from some first principles of quantum mechanics and hence provide the true explanation of why nuclei are deformed; furthermore, to give qualitative estimates for various nuclear-shell-structure effects as well as to enable a solid understanding of what is the role of shell structure in extreme conditions of nuclear dynamics at larger deformations, higher excitations and in super-heavy nuclides. Balian and Bloch (1972) were the first to recognize the connection between nuclear shell structure and the semi-classical quantization of motion in a three-dimensional well which they have formulated. It could not, therefore, answer the intriguing questions related to deformed nuclei. Another technique—Feynman's path-integral method—has provided a more general solution. The earlier calculations by Gutzwiller (1967, 1971) along this line were extended (Strutinsky 1975; Strutinsky and Magner 1976; Magner 1978) to the case of hamiltonians with certain degrees of symmetry, where continuous families of classical periodical orbits appear. This extension made it possible to analyse the shell structure in deformed potentials and to find closed solutions for such important particular cases as the general spherical potential (Strutinsky 1975; Strutinsky and Magner 1976), the deformed harmonic oscillator (Strutinsky and Magner 1976; Magner 1978), and the ellipsoidal square well (Strutinsky *et al* 1977).

In accordance with the conclusions of Balian and Bloch, the distance between the shells is determined by a condition which is similar to the familiar Bohr-Sommerfeld quantization rule, i.e.

$$\Delta e(\equiv \hbar\Omega) = \frac{2\pi\hbar}{dS_\beta(e)/\mathrm{d}e} = 2\pi\hbar/T_\beta. \tag{1}$$

Here, $S_\beta(e)$ is the action integral for the β-th family of, in general, degenerate periodical classical paths in the three-dimensional well, and

$$T_\beta = \mathrm{d}S_\beta(e)/\mathrm{d}e \tag{2}$$

is the period of rotation. In contrast to the Bohr-Sommerfeld rule, condition (1) does not determine positions of specific eigenenergies. It gives, instead, the distribution of the shells, i.e. of the zones of allowed energies in the phase space of the particle. The two rules are identical only in the exceptional cases of completely degenerate classical problem, such as the one-dimensional well, the hydrogen-like atom or the harmonic oscillator with all partial frequencies related as ratios of integer numbers. Equation (1) is the true extension of the one-dimensional Bohr-Sommerfeld quantization to three-dimensional problems which could not be found in treatises dealing with the subject: The traditional extension of the semi-classical quantization to many dimensions is not relevant since it ignores any special feature due to the appearance of periodical paths in the many-dimensional space. (Note, for example, that the textbook theory does not, at all, consider the apparent condition of periodicity, i.e. that the partial frequencies should be related as ratios of integer numbers.) In contrast to the textbook case, condition (1) characterizes the properties of the averaged-eigenvalue distribution and is related neither to properties of specific energy levels nor to the corresponding wavefunctions and quantum-mechanical quantities such as parity, orbital momentum or spatial distributions related to these. This is so because the very notion of classical paths requires a consideration of wave packets that extend over many quantal states. As an example, the solution for the spherical square well potential can be given (Balian and Bloch 1972; Strutinsky 1975; Strutinsky and Magner 1976). The major contributions to the shell structure are made by the orbits in the form of triangle- and square-shaped polygons which by no means resemble the density distributions or the l-values of the familiar wavefunctions in the quantal problem. The shell-spacing parameter $\hbar\Omega$ obtained from relation (2) for such orbits is in good agreement with the value known for the semi-empirical nuclear potentials. On the other hand, the shell energies as well as the shell component of the level density derived from the general theory are in close agreement with the values obtained for the spherical square well by the traditional numerical technique (figure 1).

It should be mentioned that it is just this feature of the new theory, i.e. considering properties averaged over quantal states, that led to relatively simple solutions in the semi-classical limit. This is the case since classical properties manifest themselves only in such averaged quantities. One should therefore distinguish between such calculations and the attempts to approximate specific quantal eigenstates.

The quantity important for the analysis of nuclear shell structure is the oscillating component of the single-particle energy distribution, which is the sum of contributions from all families of periodic paths

$$g_{\mathrm{osc}}(e) = \sum_{\beta} g_{\mathrm{osc}}^{(\beta)}(e). \tag{3}$$

In each component, the main period is as in relation (1), and the amplitude is determined by such properties of the classical problem as the number of the degrees of freedom (the classical degeneracy D), which specifies a single path in the continuous family of classical periodical orbits with the same action integral S_β, the stability of the orbit and the volume in the phase space occupied by the family of the orbits. The integer number D is restricted by the degree of phase-space symmetry of the hamiltonian, and it also cannot exceed a maximum of $2n - 2$, where n is the number of dimensions. In the case of maximum symmetry, all classical trajectories are periodical orbits, and families of orbits may exist in three-dimensional space with D up to four. In

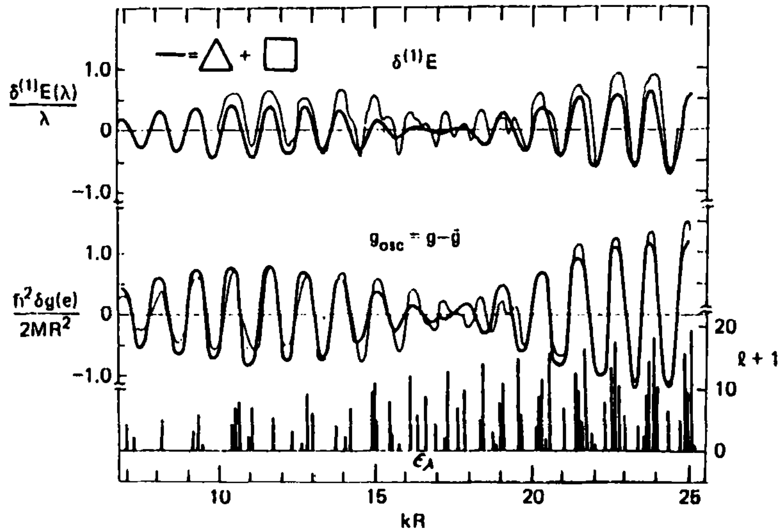

Figure 1. Eigenvalues for spherical, infinitely deep potential and their quantal degeneracy (bottom). Oscillating component of level density calculated by numerical averaging and—bold lines—by quasiclassical approximation (centre). Shell energy δE found numerically and in semi-classical approximation (bold line) in accordance with expression (4).

the one-dimensional well, $D_{max} = 0$, which puts this case among other examples of completely degenerate classical motion.

For the energy derivations the quantity of interest is not g_{osc} itself but, rather, the related component of the single-particle energy which turns out to be given by (Strutinsky 1975; Strutinsky and Magner 1976).

$$\delta E = \sum_{\beta}\left(\frac{\hbar}{T_{\beta}}\right)^{2} g_{osc}^{(\beta)}(\mu_N) = \sum_{\beta}\left(\frac{\hbar\Omega_{\beta}}{2\pi}\right)^{2} g_{osc}^{(\beta)}(\mu_N), \tag{4}$$

$$\cong \sum_{\beta}\left(\frac{\hbar v_{\beta}(\mu_N)}{L_{\beta}}\right)^{2} g_{osc}^{(\beta)}(\mu_N). \tag{5}$$

Here, μ_N is the Fermi energy for the given number N of particles, and L_β is the mean length of the β-th periodical paths. Through formulas (4) and (5), the shell energy δE is expressed in terms of classical quantities. The quantity δE is expressed in terms of classical quantities. The quantity δE plotted in figure 1 was derived from formula (4) with $g_{osc}^{\beta}(e)$ and Ω_β corresponding to the triangle- and square-shaped orbits in the spherical well.

The shell energy is approximately proportional to

$$\hbar^{-D/2} \propto (k_F R)^{D/2} \approx 2^{D} A^{D/6}, \tag{6}$$

where A is the atomic number. This explains why a more pronounced shell structure can be found in cases of higher symmetry. No less important is, however, the fact that, according to relations (4) and (5), contributions to the shell energy decrease abruptly with increasing length of the orbits (also because of the diminished stability of the lengthier orbits) and with decreasing volume occupied by the orbits. Hence, only the shortest stationary orbits not too close to the perimeter of the well are of importance for the analysis of the shell structure. This, of course, simplifies the problem essentially, at the same time making the conclusions more reliable.

The general theory sets the following conditions for a certain shape to be in equilibrium, such as the ground state or a shape isomer:

(i) The shell distribution should correspond to the condition of minimum level density at the Fermi level (closed shell or the magic nucleus!): According to relations (4) and (5), the shell structure reduces the total energy in this case;
(ii) the intensity of the shell structure must be maximal. The most important condition for this to hold true is the presence of simple, short, periodical orbits of reasonably high degeneracy.

The second condition should be clarified. Although δE increases exponentially with D, as in relation (6), in real nuclei with $k_F R \sim 10$ degeneracy and simplicity of the orbits play comparable roles and often less degenerate, but simpler orbits determine the shell structure (Strutinsky *et al* 1977). This is true for the not too strongly deformed, axially symmetric harmonic oscillator. In realistic potentials, the shell structure leading to stable deformed shapes of nuclei in their ground states—the first well in the deformation energy—is due to the presence of periodical, rhomboid-shaped paths in the axis-of-symmetry plane with $D = 2$. No analogous families of classical paths exist in the deformed harmonic oscillator. There, the main contributions to the shell energy are made by the Lissajous figures in the plane perpendicular to the symmetry axis.

The difference is reflected in the positions of the shell minima in the familiar contour diagrams showing the distribution of the shell energies (figure 2). For not too strong distortions, the slopes of the minima valleys in the ellipsoidal square well and also in the Woods-Saxon potential are opposite to that derived for the deformed harmonic oscillator. This can be explained now as due to the fact that the rhomboids are stretched and elongated, and that the action integral increases with deformation. In contrast, the above mentioned Lissajous trajectories in the harmonic oscillator shrink and the action integral decreases under the same conditions. The theory gives, however, somewhat more than just a qualitative consideration. Indeed, as long as only one type of orbit contributes to the shell energy in expression (4), it can be expected that the positions of the extrema of the shell energies as shown in figure 2 will follow the lines of constant action-integral value

$$S_\beta(\mu_N, \eta) = \text{const}, \tag{7}$$

where g_{osc} is extremal. Here and in figure 2, η is the deformation parameter and $\eta = 1$ corresponds to the spherical shape. From expression (7), the slope of the extreme line in (μ, η)-space is found to be

$$\mathrm{d}\mu/\mathrm{d}\eta = (-\,\partial S/\partial\eta)/(\partial S/\partial\mu). \tag{8}$$

For contour diagrams showing the shell energies as functions of N and η, the slope is found as

$$\mathrm{d}N/\mathrm{d}\eta = \tilde{g}(\mu_N)(\mathrm{d}\mu/\mathrm{d}\eta). \tag{9}$$

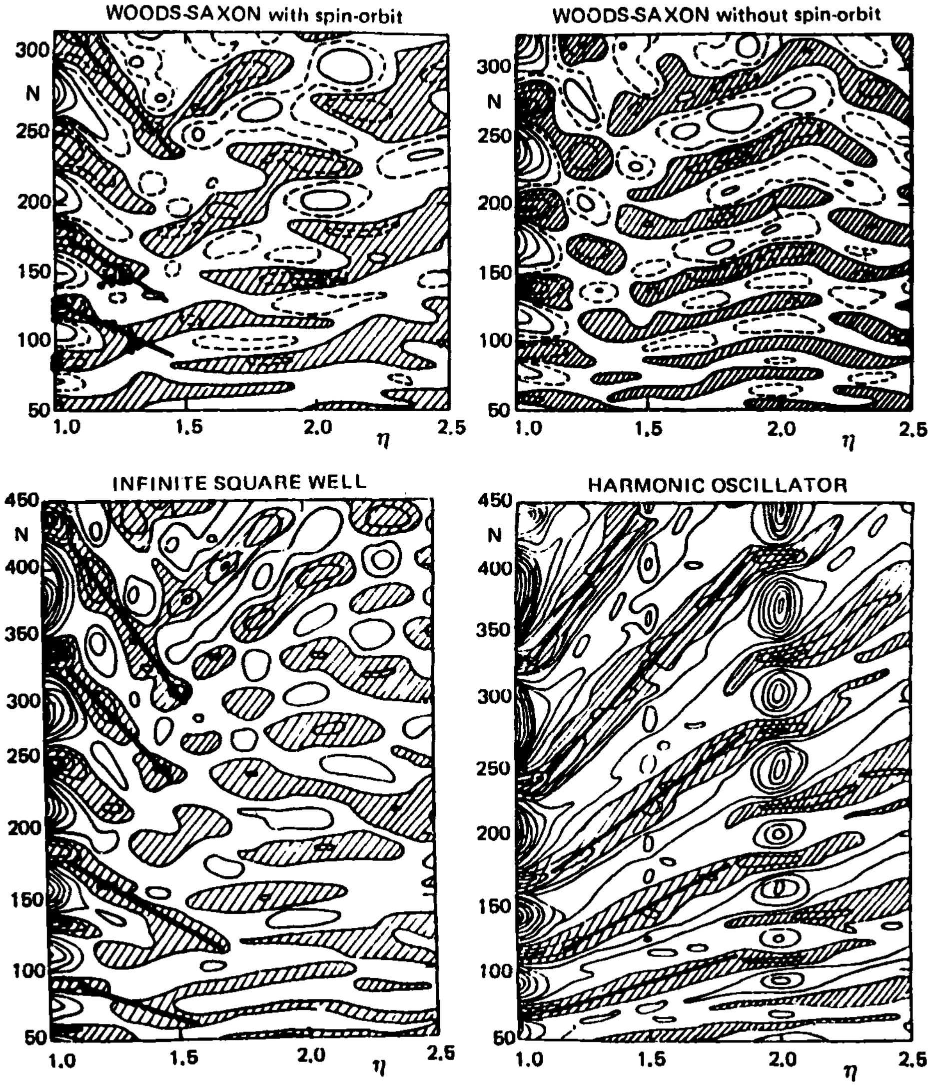

Figure 2. Shell energies $\delta E(N,\eta)$ derived numerically with potentials as indicated. Bold solid lines designate positions of minimum valleys obtained for two-fold degenerate ($D = 2$) planar families of classical orbits in the plane of the symmetry axis for the ellipsoidal, infinitely deep well (also plotted in the Woods-Saxon diagram) and in the perpendicular plane for the axially deformed harmonic oscillator. Black dots in the left-hand upper diagram are experimental values of nuclear deformations in the ground states and in the second well (from Strutinsky *et al* 1977).

For the family of rhomboids with $D = 2$ in the ellipsoidal square well, we obtain (for $\eta \approx 1$)

$$\mathrm{d}\mu/\mathrm{d}\eta = (-\mu/3\eta) < 0 \tag{10}$$

and, correspondingly,

$$\mathrm{d}N/\mathrm{d}\eta = -\tfrac{1}{2}N. \tag{11}$$

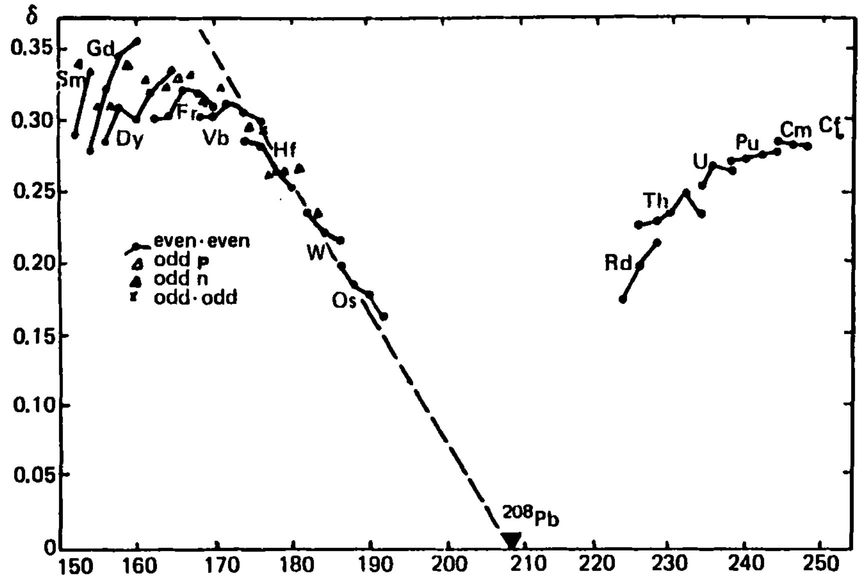

Figure 3. Quadrupole deformations of heavy nuclei. The broken line is drawn with slope given by expression (11) corresponding to rhomboid-shaped orbits in the axis-of-symmetry plane. The actinide region is too narrow for comparison (see also figure 2).

The Lissajous figures in the plane perpendicular to the symmetry axis give for the harmonic oscillator

$$d\mu/d\eta = (\mu/3\eta) > 0 \tag{12}$$

and

$$dN/d\eta = \mu^3/3(\hbar\omega_0)^3\eta. \tag{13}$$

The fat solid lines in figure 2 mark the positions of the minima of the shell energies obtained from relations (8)–(13). The agreement with the numerical calculations is remarkable. From the same simple arguments an estimate for the nuclear ground-state quadrupole deformations follows directly. The broken line in figure 3 is drawn with slope (11), and it agrees with the data in the rare-earth region (see also the discussion in (Strutinsky *et al* 1977)). So the shell structure related to planar orbits determines shell minima of energy surfaces at smaller distortions around the spherical shape.

This catholic heresy in the orthodox traditions on the origin of the nuclear deformations also led to the conclusion that it was not correct to relate the minima in the nuclear energy surface to special degeneracies in the harmonic-oscillator well. Special shapes of the harmonic potential do, indeed, provide conditions for the existence of families of orbits of the highest degeneracy with $D=4$. However, for smaller deformations—except for the spherical shape itself—the lengths of such orbits are strongly increased: to adjust two, only slightly differing frequencies, one has to go to higher harmonics, which result in longer periods of rotations and, consequently, smaller contributions to the shell energy (4). (In the harmonic oscillator the periods T_β for such highly degenerate orbits decrease as $(\eta-1)^{-1}$ near the spherical shape where $\eta \to 1$). This can be recognized as a common qualitative feature. In the general case, periodic non-planar paths appear only at very large distortions of the order of 100% and at these large distortions a new—or additional—structure appears. The shortest and therefore the most contributing among non-planar orbits are those with the partial frequencies (such as ω_φ and ω_u in the ellipsoidal square well) related as 2:1. They are considered as making the main contributions to the shell structure, leading to the second well in the deformation energy surface and to the double-humped fission barrier. Such orbits appear when the deformation approximately reaches the value of 2:1. This is not related to the special harmonic-oscillator degeneracies in the average nuclear potential. In fact, the realistic shells need not have the same strength as those observed in the harmonic oscillator at a 2:1 axis ratio. A reasonable degeneracy of $D = 2$, i.e. that of the rhomboids in the ellipsoidal well, would be sufficient to provide the shell structure which is observed in realistic nuclei in connection with fission.

An important difference with the harmonic oscillator is that, in general, the partial frequencies are not uniquely related to the shape parameters. Consequently, the three-dimensional orbits of the required type can be found for all shapes starting at around a deformation of 2:1, in contrast to the harmonic oscillator, where they arise just at this particular axis ratio. Figure 4 illustrates the appearance of the planar and three-dimensional families of periodical orbits in the ellipsoidal square-well potential and also their estimated contributions to the shell energy. The data there show that not only the deformation where the second minimum occurs but also the strength of the shell structure required for the double-humped barrier can be explained in this way.

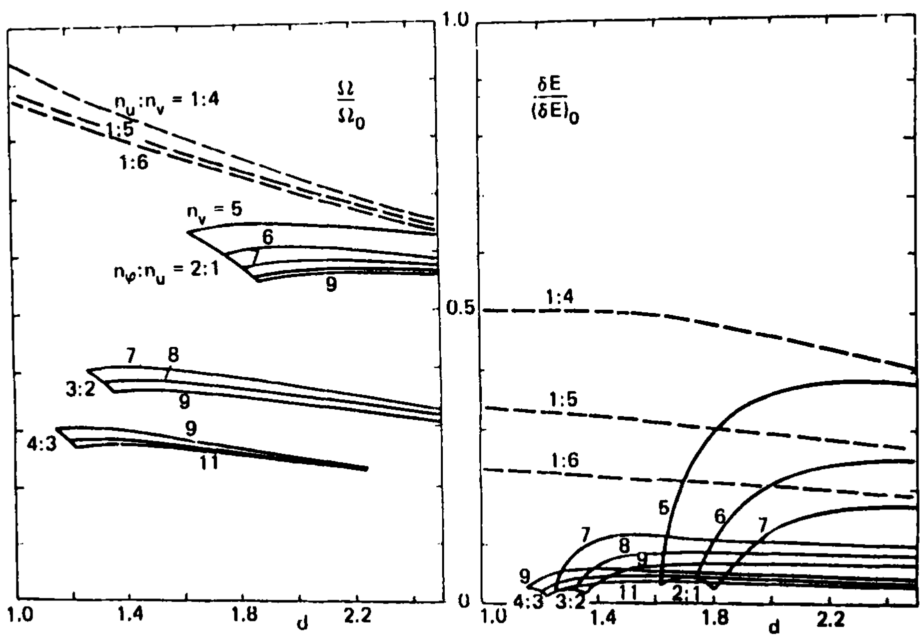

Figure 4. Rotation-frequencies Ω_β for the shortest periodical orbits in the axially symmetric infinitely deep ellipsoidal well; solid and broken lines are for the non-planar and planar paths, respectively (left); estimated shell energy contributions (right). With the curves the ratios $\omega_\varphi:\omega_u$ of the two partial frequencies are shown; this is analoguous to the $\omega_\perp:\omega_\parallel$ ratios (but not as shape parameter!) in the harmonic oscillator.

At the still larger distortions corresponding to the second barrier and close to the scission point, the shell structure is the result of a complex superposition of contributions of stationary paths of rather different kinds and it allows for an easy—but also too ambiguous—qualitative explanation of the third well, as well. Such a minimum occurs systematically in the calculations of the fission barrier in the thorium region and in lighter isotopes of uranium and plutonium (see figure 6 of Möller and Nix 1974). A simpler picture may arise after the neck has been formed: It can be assumed that at this stage of the fission process the necked shape of the nucleus does not allow the occurrence of any rhomboidal or other simple orbits crossing the nucleus from one end to the other. Instead, periodical paths constrained within either half of the nucleus become important and a transition to the shell structure in the fragments being formed takes place. In contrast to the whole-nucleus shell structure which apparently emphasizes symmetry, asymmetric shapes are now generally preferred. Within the model of two touching spherical wells, this problem has been approached by Bonche (1972).

The general theory also sheds some new light on other aspects of the shell effects in fission. One of these effects is the transition to the classical droplet model limit at higher excitations. The temperature at which this transition takes place was found to be equal to

$$T_{\mathrm{crit}} = \frac{1}{2\pi}\hbar\Omega = 1 \text{ MeV}, \tag{14}$$

where $\hbar\Omega$ is given by relation (1). This value is in good agreement with the numerical calculations (Moretto 1972; Ramamurthy *et al* 1970; Brack and Quentin 1974). It turned out, however, that, in the intermediate excitation range, the very notion of potential energy of deformation fails: Instead of a fission barrier, one deals here with the amount of work required to fission the nucleus, and this thermodynamic problem cannot be reduced to a mechanical—or a hydrodynamic—hamiltonian with characteristic potentials, forces etc. The extreme cases of very low or very high excitation energies are the only exception to this (Strutinsky and Kolomietz V M 1973). Some new aspects were also found in the problem of shell structure in the density of neutron resonances (Strutinsky 1975; Strutinsky and Magner 1976).

The general theory outlined here was not intended and does not pretend to replace the numerical derivations in obtaining quantitative results on the process of nuclear fission. For this purpose, several more effective numerical methods are available by now. Some of these methods are elaborations of the originally suggested method of energy-averaging. Other methods are based on different principles. By now, a new effective technique has been developed for finite-depth potentials, even when the Fermi evergy is only a few MeV below the edge of the well. But this development has required clarification of some points in the theory of heavy nuclei treated as nearly macroscopic systems.

An important development in fission barrier calculations has been taking place since the breakthrough in the Hartree-Fock calculations. It has also contributed significantly to establishing the questioned accuracy of the shell correction expansion. This subject is partly dealt with in the review paper by Brack (1980). What is described in the rest of this paper refers to the traditional approach and, in particular, to those of its aspects that are most closely related to the question:

3. What are the shell model potential and the nuclear shape?

Apparently, the accuracy of the energy expansion depends on the quality of the shell model potential used in the calculations. Convergence requires what may be called the statistical self-consistency between the shell model potential and the spatial density distribution (Brack and Quentin 1975): The statistically-averaged shell model density distribution ρ_s should be the same as the original (not self-consistent) smoothed distribution $\bar{\rho}$ which presumably generates the shell model potential $\bar{V}$:

$$\bar{V}(r_1) = tr_2(t(1,2)\bar{\rho}(1,2)) = tr_2[t(1,2)\tilde{\rho}_s(1,2)]. \tag{15}$$

Here, $t(1,2)$ is the effective nucleon–nucleon interaction. The second-order term in the energy expansion is given by (Strutinsky and Kolomietz 1973)

$$\delta^{(2)}E = \tfrac{1}{2}\delta\rho_s\tilde{\Gamma}\delta\rho_s + \delta\rho_s\tilde{\Gamma}(\tilde{\rho}_s - \bar{\rho}). \tag{16}$$

Here,

$$\delta\rho_s = \rho_s - \tilde{\rho}_s \tag{17}$$

and ρ_s is the density matrix corresponding to the shell model problem with the potential of the given shape. In expression (16), $\tilde{\Gamma}$ is the statistically-averaged self-consistent effective scattering amplitude. The condition (15) of the relaxed statistical consistency makes the second term in expression (16) vanish for all nuclear shapes. The second-order energy term, so far neglected in most of the calculations, is then determined entirely by the nucleon forces and the magnitude of the difference between the actual and the statistically-averaged shell model density matrices (17). The consistency requirement (15) is a very natural condition, namely, that the density distribution in the deformed potential should follow the shape of the potential. It is, however, quite clear that this condition is met with different degrees of accuracy in different phenomenological shell model potential which were designed irrespective of this criterion. Quantitatively, the role of condition (15) is described in Brack's (1980) paper within the framework of the Hartree-Fock theory.

To satisfy the statistical self-consistency condition might be much easier than to go through the original Hartree-Fock routine, and the combined semi-classical development might prove to be rather fruitful. The shell correction approach suggests, however, yet another way of handling the problem. Instead of the total rejection of the phenomenological shell model potential (as the popular Hartree-Fock way of thinking goes) one might try to exploit it as some valuable initial approximation and to correct it in such a way that condition (15) is met with sufficient accuracy. In the first order, the statistically self-consistent potential is

$$\tilde{V}_c = \bar{V} + tr_2[\tilde{\Gamma}(\tilde{\rho}_s - \bar{\rho})], \tag{18}$$

where $\bar{V}$ is any of the commonly used shell model potentials. Other forms of this equation can be found in (Strutinsky 1975). The corrected potential has the following remarkable feature: It is stationary with respect to the selection of the original potential, i.e. (18) would give approximately the same quantity no matter whether the Woods-Saxon or the Nilsson potential were in the input. Also, the nucleon force in (18) need not be as sophisticated as the one used in the Hartree-Fock calculations because the whole self-consistency routine need not be carried through. Instead, a simpler interaction can be used more suitably in reproducing the features essential for the shell corrections such as, for example, the structure at the diffuse nuclear surface. Unfortunately, little has been done along this line, as yet.

The effort undertaken to clarify the higher-order terms in the shell correction expansion has emphasized the fact that not only the smoothed energy, but also all other quantities appearing in the theory, such as shell correction energy, single-particle potential as well as the very notion of nuclear shape should rather be interpreted as macroscopic quantities defined by averaging over many intrinsic quantal states. The single-particle part of the deformation energy is the quantity averaged over a number of subsequent level crossings or particle-hole distributions. For example, the driving force due to the shell structure was found equal to

$$F_\eta = -\partial\delta E/\partial\eta = tr\left(\tilde{\Gamma}\frac{\partial\rho_0}{\partial\eta}\right), \tag{19}$$

where $\partial\rho_0/\partial\eta$ is the derivative of the averaged diagonal part of the density matrix due to the variation of the occupation numbers under deformation. No such effects are accounted for in the perturbation-based microscopic theories which assume that the given particle-hole distribution does not change. The characteristic deformation which causes the re-distribution of the particle and hole states can be estimated rather easily because both the mean slopes of the levels in the Nilsson diagram and the distance between the levels are well known. Up to the sign, the first item is of the order of the Fermi energy per unit of the quadrupole deformation, and the second one is the Fermi energy divided by A. Thus, the mean level crossing deformation is given by

$$\eta^* \approx \frac{1}{A} = 0{\cdot}01 - 0{\cdot}03. \tag{20}$$

It is easy to check that (20) agrees with what is actually seen in the Nilsson diagrams in strongly deformed nuclei. The quantity (20) is, however, so small that hardly any significance can be assigned to what happens within such a range of quadrupole deformation. On the other hand, quantities derived by the shell correction method become only significant as averages over a sufficient number of such re-distributions, which makes them appropriate to be used in the theory of processes where the amplitudes significantly exceed the characteristic deformation (20). Fission is one example of such large-amplitude macroscopic collective modes, which are the general feature of heavy nuclei, particularly at higher excitation energies. Dipole resonances or neutron shape resonances in heavy nuclei may also be recalled as examples of such modes. In all such cases, transition to the classical regime takes place, and collective states can only be seen in properly-averaged quantities like the densities of certain states or strength functions.

These arguments are in line with the general definition of macroscopic-level quantities as statistically averaged over ensembles of microscopic states. Macroscopic quantities are introduced in order to achieve a coarse-grain description of systems dynamics by inter-relating different macroscopic variables. With this definition it is obvious that macroscopic quantities and dynamics may appear only in what may be considered as microscopically poor resolution experiments. In human practice such is the vast majority of experiments because the system under study consists of such an enormous number of particles that the individual microscopic states cannot be resolved.

However in nuclear physics the standard is a microscopic experiment and the situation is just the opposite in many respects. To observe macroscopic behaviour one must sometime perform a kind of averaging over many very fine detailed microscopic data, in this way artificially creating conditions of a macroscopic experiment. This may help to understand the unusual background of nuclear theoreticians workfield. Neither completely microscopic nor macroscopic approaches may satisfy nuclear physicists dealing with complex nuclei and processes of re-arranging of many nucleons. The theory of processes in complex nuclear systems has to combine consistently the two levels of physical description, which makes it a rather unusual task in theoretical physics. Nuclear fission is a nuclear macroscopic process which is strongly affected by microscopic quantal properties among which the gross-scale non-uniformity of the nucleon phase space appears most important. The shell correction approach suggests a development along these lines and there is a hope that the experience gained in studies of the fission may, also in this way, be valuable to present and future developments.

References

Balian R and Bloch C 1971 *Ann. Phys.* **63** 592
Balian R and Bloch C 1972 *Ann. Phys.* **69** 76
Bonche P 1972 *Nucl. Phys.* **A191** 609
Brack M 1980 in *Physics and chemistry of fission* Proc. Symp. Jülich 1979 IAEA Vienna Vol. 1 p. 227
Brack M, Damgaard J, Jensen A S, Pauli H C, Strutinsky V M and Wong C Y 1972 *Rev. Mod. Phys.* **44** 320
Brack M and Quentin Ph 1974 *Phys. Scr.* **A10** 163
Brack M and Quentin P 1975 *Phys. Lett.* **B56** 421
Gutzwiller M 1967 *J. Math. Phys.* **8** 1979
Gutzwiller M 1971 *J. Math. Phys.* **12** 343
Magner A G 1978 *Yad. Fiz.* **28** 1477
Moller P and Nix J R 1974 *in Physics and chemisty of fission Proc. Symp. Rochester*, 1973, IAEA Vienna, Vol. 1 103
Moretto L G 1972 *Nucl. Phys.* **A180** 337
Moretto L G 1972 *Nucl. Phys.* **A182** 641
Nilsson S G, Tsang C F, Sobiczewski A and Szymanski Z 1969 *Nucl. Phys.* **A131** 1
Nix J R 1972 *Annu. Rev. Nucl. Sci.* **22** 65
Ramamurthy V S, Kapoor S S and Kataria S K 1970 *Phys. Rev. Lett.* **25** 386
Strutinsky V M 1975 *Nukleonika* **20** 679
Strutinsky V M 1975 *Nucl. Phys.* **A254** 197
Strutinsky V M and Magner A G 1976 *Sov. J. Part. Nucl.* **7** no. 2 138
Strutinsky V M, Magner A G, Ofengenden S R and Dossing T 1977 *Z. Phys.* **A283** 269
Strutinsky V M and Kolomietz V M 1973 *Shell structure and fission* (*Proc. Eight Winter School on Nuclear Physics*) Vol. 2 p. 483